Study of ligand substituent effects on the rate and stereoselectivity of lactide polymerization using aluminum salen-type initiators

Pimpa Hormnirun, Edward L. Marshall, Vernon C. Gibson*, Robert I. Pugh, and Andrew J. P. White

Department of Chemistry, Imperial College London, South Kensington Campus, London SW7 2AY, United Kingdom

Edited by Tobin J. Marks, Northwestern University, Evanston, IL, and approved June 26, 2006 (received for review April 5, 2006)

A series of aluminum salen-type complexes [where salen is *N*,*N*′-bis(salicylaldimine)-1,2-ethylenediamine] bearing ligands that differ in their steric and electronic properties have been synthesized and investigated for the polymerization of *rac*-lactide. X-ray crystal structures on key precatalysts reveal metal coordination geometries intermediate between trigonal bipyramidal and square-based pyramidal. Both the phenoxy substituents and the backbone linker have a significant influence over the polymerization. Electron-withdrawing groups attached to the phenoxy donor generally gave an increased polymerization rate, whereas large *ortho* substituents generally slowed down the polymerization. The vast majority of the initiators afforded polylactide with an isotactic bias; only one exhibited a bias toward heteroselectivity. Isoselectivity generally increases with increased flexibility of the backbone linker, which is presumed to be better able to accommodate any potential steric clashes between the propagating polymer chain, the inserting monomer unit, and the substituents on the phenoxy donor.

catalysis | polyesters

In recent years, Al(salen) complexes [where salen is *N*,*N*′-bis(salicylaldimine)-1,2-ethylenediamine] have been widely investigated for their ability to initiate the stereocontrolled polymerization of lactide (LA) (1–17) to give a material, polylactide (PLA), which has a range of biomedical, pharmaceutical, and agricultural applications (18–21). A convenient synthetic route to PLA is the ring-opening polymerization (ROP) of LA, the cyclic diester of lactic acid, which is derivable from renewable resources such as corn starch, sugars, and dairy produce. Metal alkoxides, for example, those of Al, Zn, Mg, Y, Ln, Sn(II), Sn(IV), Fe(II), and Fe(III), are typically used to catalyze the ROP of LA and related cyclic esters. Several reviews describing the mechanism of ROP and the types of initiators and catalysts have been published recently (22–27).

Following initial findings that simple (salen)Al complexes such as **I–III** (Fig. 1) could initiate a relatively controlled polymerization of *rac*-LA to moderately isotactic PLA (1, 2), interest developed in the potential of such initiators to mediate the stereoselective polymerization of *rac*-LA by exploiting chiral ligand backbones. Thus, the enantiomerically pure chiral aluminum complex, (***R***)**-IV**, was shown to selectively consume *D*-LA from a racemic mix ($k_D/k_L = 20$) to give optically active isotactic poly(*D*-LA) (9). The related derivative, (***R***)**-V**, was exploited to obtain syndiotactic PLA from *meso*-LA with an enantiotopic selectivity of 96% (10, 11). By using the optically inactive racemate, (***rac***)**-VI** (12, 13), a tapered stereoblock copolymer was obtained from *rac*-LA. A polymer-exchange mechanism was proposed where each enantiomer of (***rac***)**-VI** preferentially polymerizes one enantiomer of *rac*-LA, but the growing chains undergo exchange at aluminum centers of opposite chirality to produce blocks composed of the other enantiomer of LA with averaged block length of 11 monomer units (12). More recently, the cyclohexane derivatives, (***R***)**-VII** and (***rac***)**-VIII**, have been shown to polymerize *rac*-LA with high isoselectivity and excellent control in both solvent-based and solvent-free polymerizations (14, 15).

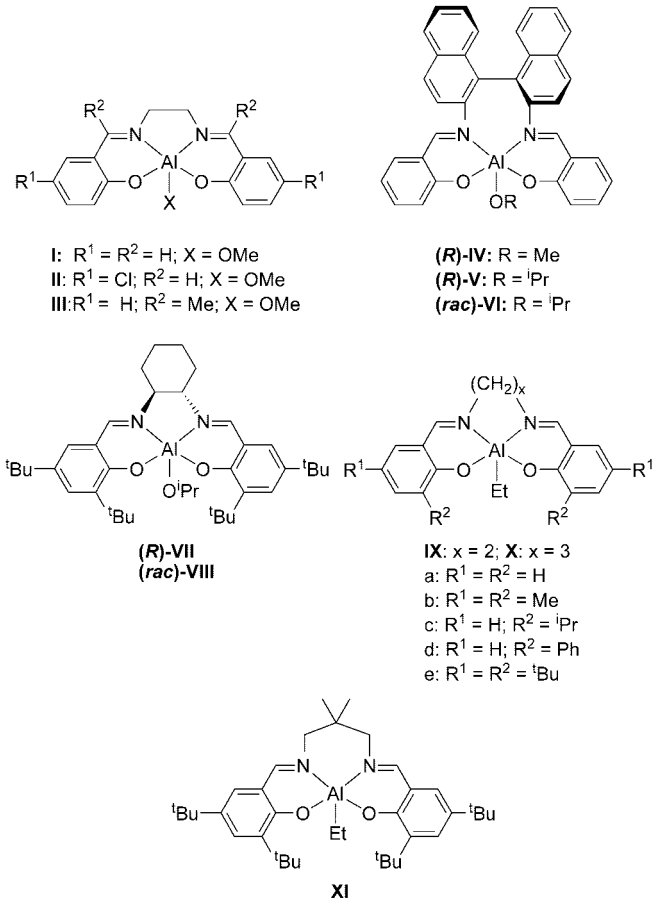

Fig. 1. Aluminum initiators and pro-initiators used in the ROP of *rac*-LA.

An interesting and potentially useful aspect of (salen)Al systems is their apparent ability to mediate isoselective polymerizations of *rac*-LA by using an achiral ligand system such as

Conflict of interest statement: No conflicts declared.

This article is a PNAS direct submission.

Abbreviations: LA, lactide; PLA, polylactide; ROP, ring-opening polymerization; salen, *N*,*N*′-bis(salicylaldimine)-1,2-ethylenediamine; TBP, trigonal bipyramidal.

Data deposition: Crystallographic data for the structures reported in this work have been deposited in the Cambridge Structural Database (CSD), Cambridge Crystallographic Data Centre, Cambridge CB2 1EZ, United Kingdom [CSD reference nos. 292440–292447 (structures **6**, **7**, **11**, **13**, **17**, **19**, **20**, and **24**, respectively)].

*To whom correspondence should be addressed. E-mail: v.gibson@imperial.ac.uk.

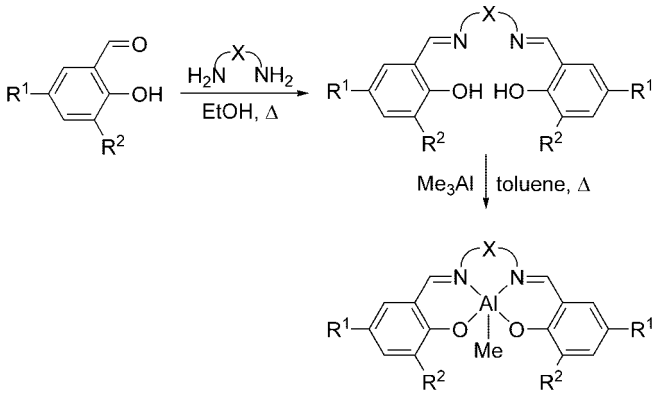

Fig. 2. Synthetic pathway for the preparation of complexes **1**–**24**.

those contained in **IX** and **X** (6). The isoselectivity is enhanced for initiators bearing more flexible C_3 linkers, and introducing large *ortho*-phenoxy substituents also was found to increase the isotacticity. Further tacticity enhancements have been reported for the dimethyl-substituted derivative **XI** (7). The mechanism of stereoselective polymerization using these achiral ligand-based complexes is postulated to operate by means of a chain end control process (6), whereas an enantiomorphic-site control mechanism is proposed for the chiral salen-based complexes (10). However, recent studies have highlighted some complexities in ascribing the mechanism to chain-end control or enantiomorphic-site control (16). The chirality of the ligand bonded to the metal, the chirality of the end group of the growing polymer chain, and the solvent all seem to play a complex and rather unpredictable role in influencing the stereopreference in a racemic monomer mixture.

With regard to the productivities of (salen)Al systems, in the rather limited number of studies to date it has been found that the rate of polymerization is enhanced by appending electron-withdrawing substituents to the phenoxide donor (4). Enhanced activities also have been observed by using a salicylketimine derivative containing neither bulky nor electron-withdrawing substituents on the phenoxide donor (5).

Although Al(salen) complexes are attractive as initiators because of their ease of preparation and the stability afforded by the tetradentate ligand, it is clear that significant gaps remain in our knowledge of the fundamental factors influencing activity and selectivity. We therefore initiated a systematic investigation into the LA polymerization behavior of a family of Al(salen) initiator systems, in which the phenoxy substituents and the length and nature of the diimino-linking units are varied, with a view to obtaining an improved understanding of the influence of salen-type ligands on the rate and stereoselectivity of *rac*-LA polymerization.

Results

Pro-Initiator Synthesis. The salicylaldimines used in this study were prepared through condensation of two equivalents of commercially available salicylaldehydes (α-hydroxybenzaldehydes) with an α,ω-diamine according to standard literature procedures (28). The salicylaldimines then were reacted with one equivalent of trimethylaluminum at 110°C for 18 h to afford the (salen)Al(CH_3) complexes in moderate to high yields according to Fig. 2. The complexes synthesized (**1**–**24**) (Fig. 3) span C_2 and C_3 backbones of varying degrees of rigidity (Groups A–F) along with two additional families containing arylene linkers (Groups G and H). Attempts to synthesize the $R^1 = R^2 = H$ and $R^1 = R^2 = Cl$ members of Group F led to intractable mixtures of low-solubility products. To the best of our knowledge, only complexes **1**, **2**, **4**, and **10** have been reported previously (29–31).

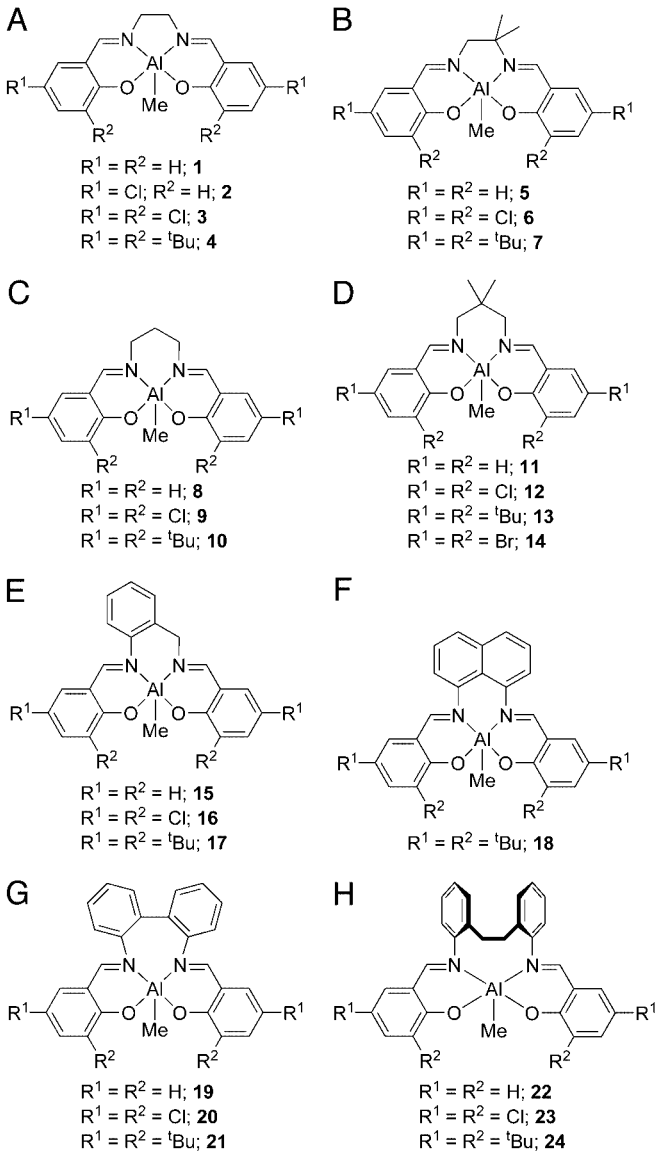

Fig. 3. Complexes **1**–**24** synthesized as part of this study from Groups *A*–*H*.

The 1,2-ethylenediamino-based complexes **1**–**7** were all obtained as yellow crystalline materials after recrystallization either directly from the reaction medium for the less-soluble examples (e.g., **3**) or from MeCN (full experimental details for complexes **1**–**24** are provided in *Supporting Text*, Figs. 10–42, and Tables 2–7, which are published as supporting information on the PNAS web site). The presence of the methyl substituents on the backbone of **5**–**7** renders these complexes significantly more soluble than their nonsubstituted counterparts, and hence recrystallized yields of these were generally lower than for **1**–**4** (e.g., 37%, **6**; 45%, **7**). The difference in solubility is particularly apparent for the dichlorophenoxy derivatives **3** and **6**, the former being insoluble in hot toluene, whereas complex **6** is soluble in room-temperature toluene solution. This observation suggests that the low solubility of other metal salen complexes, a problem commonly encountered with such species, may be rectified by introducing alkyl groups onto the diimino linker.

The ^{1}H NMR spectra of complexes **1**–**4** all feature complex second-order multiplets in the region δ 2.0–4.0 for the protons

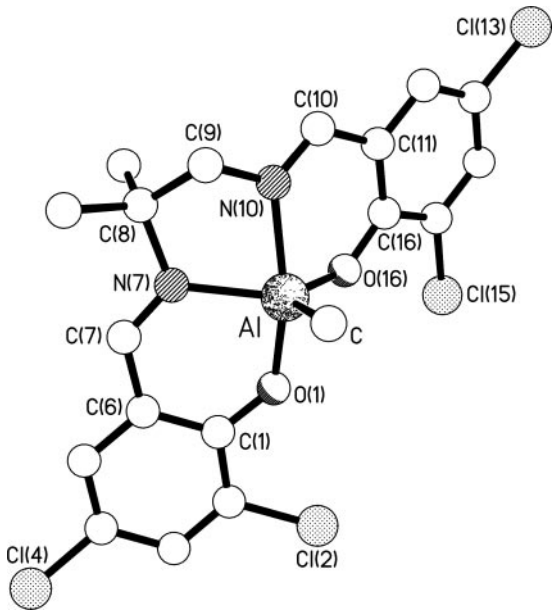

Fig. 4. Molecular structure of **6**. Selected bond lengths (Å) and angles (°) are as follows: Al–C 1.949(7); Al–O(1) 1.825(4); Al–N(7) 1.997(5); Al–N(10) 2.042(5); Al–O(16) 1.808(4); C(7)–N(7) 1.290(9); N(10)–C(10) 1.293(9): C–Al–O(1) 103.2(3); C–Al–N(7) 110.7(3); C–Al–N(10) 94.9(3); C–Al–O(16) 120.8(3); O(1)–Al–N(7) 90.3(2); O(1)–Al–N(10) 161.0(2); O(1)–Al–O(16) 89.4(2); N(7)–Al–N(10) 77.8(2); N(7)–Al–O(16) 127.2(2); N(10)–Al–O(16) 86.2(2).

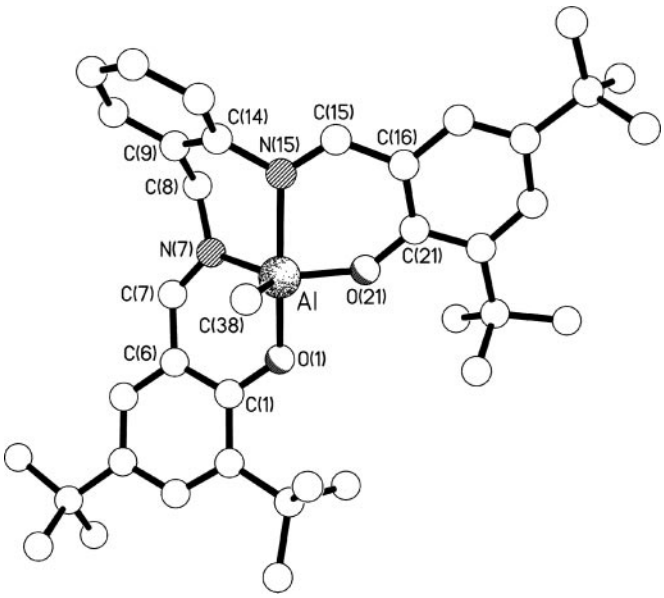

Fig. 5. Molecular structure of **17**. Selected bond lengths (Å) and angles (°) are as follows: Al–O(1) 1.835(2); Al–N(7) 1.995(2); Al–N(15) 2.096(2); Al–O(21) 1.786(2); Al–C(38) 1.958(3); C(7)–N(7) 1.288(4); C(15)–N(15) 1.289(4): O(21)–Al–O(1) 89.09(8); O(21)–Al–C(38) 122.74(14); O(1)–Al–C(38) 99.77(11); O(21)–Al–N(7) 121.60(10); O(1)–Al–N(7) 88.72(9); C(38)–Al–N(7) 115.10(13); O(21)–Al–N(15) 87.32(9); O(1)–Al–N(15) 168.79(10); C(38)–Al–N(15) 91.09(11); N(7)–Al–N(15) 84.14(9).

of the ethylene backbone, consistent with diastereotopic methylene environments. The observation of just one imine environment in their ^{1}H and ^{13}C NMR spectra is consistent with fluxional behavior. For complexes **5**–**7**, the unsymmetrical nature of the 1,1-dimethyl-1,2-ethylene backbone expectedly affords inequivalent phenoxide rings and two imine proton resonances.

Syntheses of the C_3-linked diamino-based complexes (**8**–**18**) also proceed in straightforward fashion. The spectroscopic data obtained on these compounds are largely unremarkable and consistent with the proposed formulations. In the ^{1}H NMR spectra of complexes **8**–**10**, **11**–**14**, and **15**–**17**, the unsubstituted backbone methylene protons again display second-order coupling effects, typically giving rise to symmetrical doublets of multiplets (**9**, **10**) or doublets of doublets (**11**–**17**), as expected for diastereotopic proton environments.

The ^{1}H NMR spectra of the diaryl-linked backbone species **19**–**21** show two ^{1}H imine singlet resonances consistent with a locked conformation; accordingly, the spectrum of **21** also features four singlets for the *t*-butyl substituents. The ^{1}H NMR spectra of complexes **22**–**24** are more complex, arising from the mobility of the ethylene linking unit, with broadened signals being observed for the ethylene bridge and the protons of the backbone arylene units.

X-Ray Crystallography. With a view to assessing whether any underlying geometrical effect imposed by the tetradentate ligand might account for the polymerization activities and selectivities, crystal structure determinations were carried out on selected complexes from Groups B, D, E, G, and H; a number of examples from Group A were available from the literature (4, 31, 32). The molecular structures of the representative complexes **6**, **17**, **20**, and **24** are shown in Figs. 4–7. The structures of complexes **7**, **11**, **13**, and **19** are included in Figs. 11, 12, and 19–27. All eight structures feature five-coordinate trigonal bipyramidal (TBP) geometries at the aluminum centers, although at varying places in the continuum from ideal square-based pyramidal [$\tau = 0$] to ideal TBP [$\tau = 1$] as described by using the τ parameter introduced by Addison *et al.* (33) (see Table 1). To a first approximation, it might be expected that there would be a correlation between τ and the bite angle of the central *N*,*N*′ chelate (the *O*,*N* chelate rings at each end of the ligands are the same in each complex, and the fifth donor is methyl in each case); because the *N*,*N*′ chelate in each complex links an equatorial donor to an axial donor, a bite angle of $<90°$ would be expected

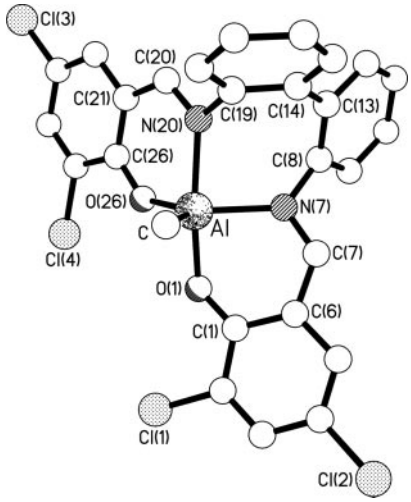

Fig. 6. Molecular structure of one (II) of the two independent complexes present in the crystals of **20**. Selected bond lengths (Å) and angles (°) are as follows: Al–C 1.976(10); Al–O(1) 1.852(6); Al–N(7) 2.053(7); Al–N(20) 2.032(8); Al–O(26) 1.792(6); C(7)–N(7) 1.312(11); N(20)–C(20) 1.327(11): C–Al–O(1) 98.7(4); C–Al–N(7) 112.4(4); C–Al–N(20) 94.7(4); C–Al–O(26) 121.5(4); O(1)–Al–N(7) 87.6(3); O(1)–Al–N(20) 166.4(3); O(1)–Al–O(26) 86.9(3); N(7)–Al–N(20) 85.5(3); N(7)–Al–O(26) 126.0(3); N(20)–Al–O(26) 87.6(3). Analogous data for **I** may be found in Figs. 15, 19, 17, and 21 and *Supporting Text*.

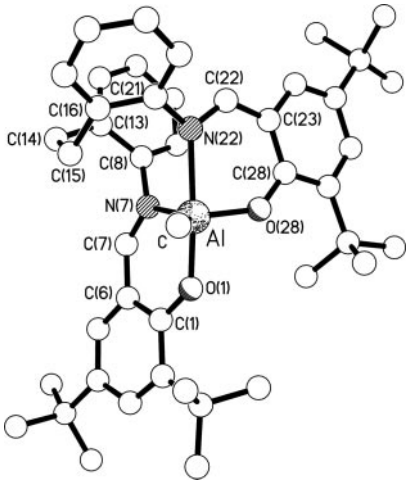

Fig. 7. Molecular structure of **24**. Selected bond lengths (Å) and angles (°) are as follows: Al–C 1.966(5); Al–O(1) 1.820(3); Al–N(7) 2.025(3); Al–N(22) 2.186(3); Al–O(28) 1.758(3); C(7)–N(7) 1.302(5); C(22)–N(22) 1.299(5): O(28)–Al–O(1) 94.9(2); O(28)–Al–C 119.3(2); O(1)–Al–C 93.6(2); O(28)–Al–N(7) 105.72(14); O(1)–Al–N(7) 88.14(14); C–Al–N(7) 134.6(2); O(28)–Al–N(22) 87.20(13); O(1)–Al–N(22) 174.32(14); C–Al–N(22) 89.9(2); N(7)–Al–N(22) 86.20(13).

to reduce the transaxial angle β and thus reduce τ. However, such a correlation is only present at the extreme ends of the τ range; complexes **6** and **7** have the smallest values of τ ($\approx$0.5) and the smallest *N*,*N*′ bite angles [$\approx$77°], and complex **19** has the largest τ (0.91) and the largest *N*,*N*′ bite angle [87.33 (12)°]. In between, the correlation is lost; complexes **20** and **24** have $\tau \sim 0.67$ with *N*,*N*′ bite angles of $\approx$86°, whereas complexes **11**, **13**, and **17** have a larger τ of $\approx$0.75 but smaller *N*,*N*′ bite angles of $\approx$84°. It is thus clear that the flexibility of the linkage between the two nitrogen centers, and thus their ability to adopt a bite angle approaching 90°, is not the sole factor affecting the geometry at the metal center. Indeed, comparing complexes **19** and **20**, which differ only in the 2,4-substituents of the salicylaldimine rings (hydrogen in **19**, chlorine in **20**), reveals bite angles that differ by $\approx$2°, β angles that vary by $\approx$6°, and τ values of 0.91 and $\approx$0.68, respectively. It is apparent, therefore, that electronic effects also play a vital role. Interestingly, changing the 2,4-substituents on the salicylaldimine from chlorine to *t*-butyl has almost no effect; comparing complex **6** (chlorine) with complex **7** (*t*-butyl) reveals almost no change in the *N*,*N*′ bite angles, β angles, or τ values. For complexes **11** (hydrogen) and **13** (*t*-butyl), the *N*,*N*′ bite angles are almost identical (different by only $\approx$0.1°), the β angles vary by $\approx$4°, and the τ values are 0.79 and 0.72, respectively. Clearly, therefore, the geometry at the aluminum centers is a result of a subtle interweaving of disparate factors, and more work will be required if these relationships are to be fully understood.

Table 1. The square-based pyramidal/TBP parameter τ for the solid-state structures of complexes 6, 7, 11, 13, 17, 19, 20, and 24

Complex	A*	α,† °	β,‡ °	τ§	N–N bite, °
6	C	127.2(2)	161.0(2)	0.56	77.8(2)
7 (I)	C	130.18(15)	160.08(15)	0.50	76.76(14)
7 (II)	C′	129.31(15)	159.67(14)	0.51	77.33(14)
11	N(7)	122.58(10)	170.09(8)	0.79	83.74(8)
13	C	123.19(10)	166.32(9)	0.72	83.62(9)
17	N(7)	122.74(14)	168.79(10)	0.77	84.14(9)
19	O(1)	118.14(19)	172.77(14)	0.91	87.33(12)
20 (I)	C	125.3(3)	166.7(3)	0.69	85.6(3)
20 (II)	C′	126.0(3)	166.4(3)	0.67	85.5(3)
24	O(28)	134.6(2)	174.32(14)	0.66	86.20(13)

*Ligand A is defined as being the donor atom not involved in the two largest angles at the metal center.
†Angle α is the second-largest angle at the metal center.
‡Angle β is the largest angle at the metal center.
§[$\tau = (\beta - \alpha)/60°$].

Polymerization Studies. Polymerizations were carried out by treatment of the methyl precursor complexes **1**–**24** with a stoichiometric equivalent of benzyl alcohol in toluene. ^{1}H NMR validation studies confirmed that the alkoxide initiating species is generated cleanly and swiftly by this procedure. The temperature of the initiator solution then was raised to 70°C ,and *rac*-LA was added. For comparative purposes, the molar ratio of *rac*-LA to initiator was fixed at 50:1 {$[LA]_0$ = 0.416 M; $[Al]_0$ = 8.33 mM; M_n (theory) = 7,200}. Polymerizations were typically allowed to proceed to high (>90%) conversion, with the exception of some of the slower systems, before termination by addition of a small amount of methanol. In each case, aliquots were removed throughout the polymerization and monomer conversion, and molecular weights were determined by ^{1}H NMR spectroscopy and gel permeation chromatography, respectively. Molecular weight, rate, and tacticity data are collected for systems containing C_2 and C_3 alkylene linkers and the phenylene-containing linkers in Figs. 8 and 9, respectively.

(i) C_2 and C_3 alkylene backbones: For initiators derived from Group A complexes containing a C_2 (ethylene) backbone, a comparison of the data for compounds **1** and **4** reveals a dramatic effect on rate upon incorporating bulky substituents at the *ortho* positions of the phenoxy donors. Thus, the initiator derived from **4** polymerizes *rac*-LA at a rate $\approx$50 times slower than that for **1**, which has protons in the equivalent positions. An enhancement of the polymerization rate due to an electronic effect is also observed. For example, comparing **1** with **3** reveals a tripling of the rate for the chloro-substituted ligand, despite the increased steric hindrance of the *ortho* chloro groups, which, to a first approximation, may be viewed as being sterically similar to methyl substituents. A smaller, although significant, rate enhancement is seen upon introducing a chloro substituent into the *para* position (compare **1** vs. **2**). The kinetic behavior of this group of catalysts is significantly different from the other groups (B–H) (see below). Higher M_n values than predicted were found at the beginning of the polymerizations (Fig. 28), due to an induction effect (Fig. 38), which equates to a poor rate of initiation. Such induction periods also have been observed for other initiator systems (34), but they do not occur for the other groups of Al(salen) initiators studied here.

All of the PLA products afforded by the Group A initiators show a bias toward isotacticity, with the *t*-butyl derivative **4** giving the highest value (83%) within this grouping. Interestingly, the 2,4-dichloro derivative (**3**) afforded the lowest bias toward isotacticity (56%), despite the presence of quite sterically demanding chloro substituents. Introducing a gem-dimethyl unit into the ligand backbone (Group B) did not afford a dramatic change in polymerization behavior compared with those in Group A, with similar trends due to H (**5**), Cl (**6**), and Bu^t (**7**) ligand substituents. The isotacticity for the *t*-butyl derivative was found to be somewhat lower (77%) than for the nonsubstituted ethylene backbone derivative **4**.

Lengthening the backbone to a C_3 alkylene linker gave rise to a dramatic increase in polymerization rate, with the highest being recorded for the dichloro derivative **9**. Comparing **1** with **8** reveals an 11-fold rate increase upon exchanging the C_2 for the C_3 linker, whereas for the *t*-butyl derivative, the increase is >2 orders of magnitude. There is also a noticeable increase in isotacticity for samples generated by the unsubstituted (**8**) and di-*t*-butyl-substituted (**10**) ligands. The chloro-substituted initiator, **9**, again shows lower stereoselectivity. Interestingly, further

A

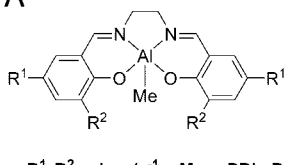

	R^1	R^2	k_{app}/s^{-1}	M_n	PDI	P_m
1	H	H	59 x 10^{-6}	4390	1.76	0.68
2	Cl	H	103 x 10^{-6}	4290	1.43	0.70
3	Cl	Cl	181 x 10^{-6}	7130	1.58	0.56
4	tBu	tBu	1 x 10^{-6}	5900	1.27	0.83

B

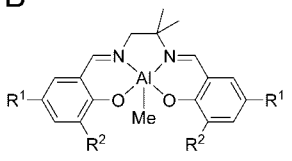

	R^1=R^2	k_{app}/s^{-1}	M_n	PDI	P_m
5	H	49 x 10^{-6}	8220	1.34	0.68
6	Cl	292 x 10^{-6}	7540	1.38	0.60
7	tBu	1 x 10^{-6}	7250	1.31	0.77

C

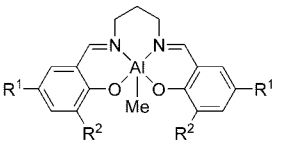

	R^1=R^2	k_{app}/s^{-1}	M_n	PDI	P_m
8	H	661 x 10^{-6}	6560	1.40	0.75
9	Cl	1009 x 10^{-6}	9700	1.08	0.60
10	tBu	133 x 10^{-6}	9590	1.07	0.88

D

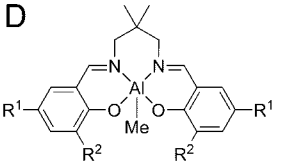

	R^1=R^2	k_{app}/s^{-1}	M_n	PDI	P_m
11	H	1073 x 10^{-6}	6190	1.35	0.63
12	Cl	6420 x 10^{-6}	7470	1.37	0.59
13	tBu	159 x 10^{-6}	7430	1.20	0.85
14	Br	3609 x 10^{-6}	8140	1.19	0.64

Fig. 8. Polymerization data for complexes **1–14**; {[LA]$_0$/[Al]$_0$ = 50; toluene, 70°C; M_n (theory) = 7,200}; errors on k_{app} values: ±5%. Data are from Groups *A–D*.

E

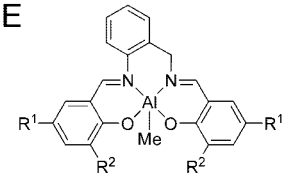

	R^1=R^2	k_{app}/s^{-1}	M_n	PDI	P_m
15	H	928 x 10^{-6}	7570	1.40	0.68
16	Cl	4380 x 10^{-6}	9320	1.13	0.63
17	tBu	84 x 10^{-6}	7920	1.08	0.86

F

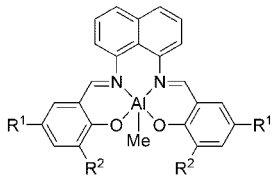

	R^1=R^2	k_{app}/s^{-1}	M_n	PDI	P_m
18	tBu	784 x 10^{-6}	10780	1.14	0.72

G

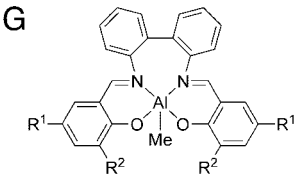

	R^1=R^2	k_{app}/s^{-1}	M_n	PDI	P_m
19	H	52 x 10^{-6}	6810	1.08	0.84
20	Cl	8 x 10^{-6}	3500	1.33	0.37
21	tBu	1 x 10^{-6}	6560	1.26	0.63

H

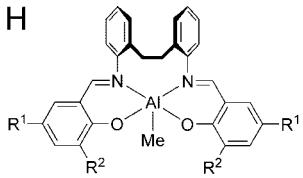

	R^1=R^2	k_{app}/s^{-1}	M_n	PDI	P_m
22	H	86 x 10^{-6}	7350	1.23	0.50
23	Cl	85 x 10^{-6}	8950	1.14	0.60
24	tBu	3 x 10^{-6}	8100	1.20	0.55

Fig. 9. Polymerization data for complexes **15–24**; {[LA]$_0$/[Al]$_0$ = 50; toluene, 70°C; M_n (theory) = 7,200}; errors on k_{app} values: ±5%. Data are from Groups *E–H*.

substantial increases in polymerization rate are seen for the gem-dimethyl–substituted C_3 backbone initiators (Group D), although the isoselectivity is diminished slightly.

(ii) Phenylene-containing backbones: For the E series of initiators, where a more rigid phenylene linker is incorporated into the C_3 backbone, a substantial enhancement of polymerization rate for the dichloro derivative **16** relative to **9** was observed, with the rates for the H and *t*-butyl derivatives being relatively comparable (compare **8** vs. **15** and **10** vs. **17**). Similarly high isotactic content PLA (86%) is obtained for the *t*-butyl derivative along with a narrow molecular weight distribution (1.08). The *t*-butyl derivative of a naphthyl linking unit (**18**) afforded a much higher activity than for all other derivatives containing the 2,6-di-*t*-butyl combination, but the isoselectivity was lowered.

For initiators containing a biphenyl linker (Group G), the activities are dramatically lowered. The unsubstituted derivative **19** gave a narrow molecular weight distribution and a remarkably high isotactic content of 84%, comparable with di-*t*-butyl derivatives attached to other backbones. Interestingly, the dichloro initiator **20** gave a significant heterotactic bias (P_r 0.63), the only derivative within this Al(salen) family of initiators to have afforded heterotactic-biased PLA, although with a significant loss over molecular weight control. As the lowering of activity and the surprising stereocontrol may be related to the rigidity of the biphenyl linker, we decided to examine complexes **22–24** in which a flexible ethylene linker connects the phenylene units. However, activities did not greatly improve, and the tacticity control was largely lost.

Discussion

From the results obtained using these initiating systems, it is apparent that the activity of each aluminum center is strongly influenced by the nature of the phenoxy substituents. For example, the 2,4-di-*t*-butylphenoxy derivatives **4** and **7** afford substantially slower propagation rates than any other member of Groups A and B. This observation is attributed to the size of the *ortho* substituents, which are believed to obstruct either the approach of the LA monomer to the aluminum center or a key transition state associated with ring-opening. This effect is seen throughout the ligand families used in the study, with rates for the complexes featuring *ortho-t*-butyl–substituted ligands consistently lower than for all other members of the same family.

An electronic effect is also apparent, with electron-withdrawing substituents attached to the phenoxy donors affording more active aluminum centers, presumably a consequence of enhanced metal electrophilicities. Hence, the halide-substituted bis(iminophenoxide) complexes typically exhibit greater polymerization activities than do their counterparts bearing unsubstituted phenoxide rings. An exception arises for complexes containing the 2,2′-diaminobiphenyl backbone where the unsubstituted derivative gave a 5-fold higher polymerization rate than that for its 2,4-dichloro relative. A similar, although less pronounced, effect is found in Group H.

The C_3 linker clearly exerts a beneficial effect on polymerization rate, which is likely attributable to the greater flexibility imparted to the metal coordination sphere and thus better accommodation of the geometric requirements of the transition state(s) for the ring-opening process. It might be expected that some aspects of these geometric effects will be apparent in the ground-state structures of the aluminum pro-initiators. A comparison of the molecular structures of the ethylene backbone complexes with their propylene backbone relatives reveals two important differences. First, the ethylene backbone complexes contain NN bite angles of ≈76–78°, whereas the longer propylene linker affords bite angles in the range 83–88°. Accordingly, the τ parameters for the C_2 linker complexes are in the range 0.50–0.56, compared with 0.70–0.79 for complexes containing the C_3 linker; i.e., there is a substantial constraint toward square-based pyramidal coordination for the ethylene-bridged compounds, whereas the propylene backbone complexes favor TBP coordination. However, a distortion toward a TBP geometry does not solely account for the rate enhancements, because the similarly TBP-biased complexes **17** and **20** gave less active catalysts. Further, complex **19**, which shows the greatest distortion toward a TBP coordination geometry (τ = 0.91), afforded quite low activity. The ^{1}H NMR data for **18–21**, however, indicate that they are "locked" and therefore without the flexibility of their C_3-alkenyl linker counterparts. It seems likely, therefore, that the enhanced performance of the C_3 backbone catalysts is more a function of the flexibility of the linking unit,

which may allow the complex to better access the key transition states involved in the ROP process. It also would appear to have a favorable effect on initiation because the initiators with C_2-linking units all display a significant induction period before the onset of polymerization.

The molecular weights of the PLA samples generally show good agreement with theoretical values in accord with a well controlled coordinative insertion process (see *Supporting Text*). Molecular weight distributions, however, broaden at higher monomer conversions, i.e., low monomer concentrations, because of transesterification side-reactions. High levels of transesterification are particularly pronounced for the smaller salen ligands, such as **1** and **2**. However, changing the backbone structure from an ethylene to a propylene linker typically leads to a marked reduction in the degree of transesterification, an effect also noted by Nomura *et al.* (6).

The origin of the isoselectivity observed by using (salen)Al initiators is less readily pinpointed from these studies. Nonetheless, some trends are apparent. For example, comparison of the P_m values for initiators from Groups A–E indicate that the nature of the phenoxy substituents is important. Systems containing *ortho-t*-butyl substituents afford the highest isoselectivities, 83 ($\pm$6) % for **4**, **7**, **10**, **13**, and **17**, whereas unsubstituted derivatives gave isoselectivities of 69 ($\pm$6) % (for **1**, **5**, **8**, **11**, and **15**). Interestingly, the 2,4-dichloro–substituted complexes, **3**, **6**, **9**, **12** and **16**, gave somewhat lower isotactic contents of 56%, 60%, 60%, 59%, and 63%, respectively, despite the presence of the sterically significant *ortho*-chloro substituent. The latter observation clearly indicates an electronic contribution to the stereochemistry of insertion.

The nature of the linkage between the imino donors is also important, with the good isoselectivities of Groups A–E contrasting with lower values for the more rigid diarylene backbone complexes of Groups F–H. Indeed, trends within Groups F–H are far less apparent than for their aliphatic counterparts, and the factors influencing stereocontrol may not be the same. For example, the unsubstituted complex **19** gave a higher isotacticity than its *t*-butyl relative, **21**, whereas somewhat surprisingly **20** gave moderate heteroselectivity; it is to our knowledge the only (salen)Al system to date to afford a heteroselective bias.

In light of the conclusions of a recent theoretical study (35), we surmise that the isotactic assembly mode is favored because steric clashes between the propagating chain, the incoming monomer, and the salen substituents are minimized (relative to heterotactic insertion) during the rate-determining transition state, and a mobile backbone would be expected to better accommodate such interactions. Preliminary results from a DFT quantum chemical study (E.L.M., V.C.G., and H. S. Rzepa, unpublished data) are in accord with this rationale and will be published elsewhere.

Conclusions

A study of the factors influencing the ROP of *rac*-LA by (salen)Al initiators has revealed several important effects as follows: (*i*) high activities are favored by electron-withdrawing substituents attached to the phenoxy-donor; (*ii*) activities are enhanced by flexible 3-carbon linkers between the imino nitrogen donors; (*iii*) activities are suppressed by large *ortho*-phenoxy substituents; and (*iv*) isoselectivity is specially favored by a combination of a flexible aliphatic C_3 linker and sterically demanding *ortho*-phenoxy groups.

Materials and Methods

Synthesis of Complexes 1–24. All ligands used in this study were prepared by the condensation reaction between two equivalents of the appropriate salicylaldehyde and one equivalent of an α,ω-diamine in refluxing ethanol. The Al complexes were prepared by stirring with $AlMe_3$ in toluene at 110°C. Full details are given in *Supporting Text*.

Polymerization Studies. To a mixture of *rac*-LA (0.72 g, 5.0 mmol) and $PhCH_2OH$ (5.2 μl, 0.05 mmol) was added a solution of catalyst (0.05 mmol) in toluene (6 ml). The reaction was stirred at 70°C with samples periodically removed for analysis. Once the conversion was >90%, the reaction was quenched with methanol (two to three drops).

P.H. was supported by a Royal Thai Government Studentship.

1. Le Borgne A, Vincens V, Jouglard M, Spassky N (1993) *Makromol Chem Macromol Symp* 73:37–46.
2. Wisniewski M, Le Borgne A, Spassky N (1997) *Macromol Chem Phys* 198:1227–1238.
3. Montaudo G, Montaudo MS, Puglisi C, Samperi F, Spassky N, Le Borgne A, Wisniewski M (1996) *Macromolecules* 29:6461–6465.
4. Cameron PA, Jhurry D, Gibson VC, White AJP, Williams DJ, Williams S (1999) *Macromol Rapid Commun* 20:616–618.
5. Bhaw-Luximon A, Jhurry D, Spassky N (2000) *Polym Bull* 44:31–38.
6. Nomura N, Ishii R, Akakura M, Aoi K (2002) *J Am Chem Soc* 124:5938–5939.
7. Tang Z, Chen X, Pang X, Yang Y, Zhang X, Jing X (2004) *Biomacromolecules* 5:965–970.
8. Tang Z, Chen X, Yang Y, Pang X, Sun J, Zhang X, Jing X (2004) *J Polym Sci Polym Chem* 42:5974–5982.
9. Spassky N, Wisniewski M, Pluta C, Le Borgne A (1996) *Macromol Chem Phys* 197:2627–2637.
10. Ovitt TM, Coates GW (1999) *J Am Chem Soc* 121:4072–4073.
11. Ovitt TM, Coates GW (2002) *J Am Chem Soc* 124:1316–1326.
12. Ovitt TM, Coates GW (2000) *J Polym Sci Polym Chem* 38:4686–4692.
13. Radano CP, Baker GL, Smith MR (2000) *J Am Chem Soc* 122:1552–1553.
14. Zhong Z, Dijkstra PJ, Feijen J (2002) *Angew Chem Int Ed* 41:4510–4513.
15. Zhong Z, Dijkstra PJ, Feijen J (2003) *J Am Chem Soc* 125:11291–11298.
16. Chisholm MH, Patmore N, Zhou Z (2005) *Chem Commun*, 127–129.
17. Majerska K, Duda A (2004) *J Am Chem Soc* 126:1026–1027.
18. Uhrich KE, Cannizzaro SM, Langer RS, Shakesheff KM (1999) *Chem Rev* 99:3181–3198.
19. Chiellini E, Solaro R (1996) *Adv Mater* 8:305–313.
20. Ikada Y, Isuji H (2000) *Macromol Rapid Commun* 21:117–132.
21. Drumwright RW, Gruber PR, Henton DE (2000) *Adv Mater* 12:1841–1846.
22. Coates GW (2002) *J Chem Soc Dalton Trans*, 467–475.
23. O'Keefe BJ, Hillmyer MA, Tolman WB (2001) *J Chem Soc Dalton Trans*, 2215–2224.
24. Nakano K, Kosaka N, Hiyama T, Nozaki K (2003) *J Chem Soc Dalton Trans*, 4039–4050.
25. Dechy-Cabaret O, Martin-Veca B, Bourissou D (2004) *Chem Rev* 104:6147–6176.
26. Chisholm MH, Zhou Z (2004) *J Mater Chem* 14:3081–3092.
27. Wu J, Yu T-L, Chen C-T, Lin C-C (2006) *Coord Chem Rev* 250:602–626.
28. Cozzi PG (2004) *Chem Soc Rev* 33:410–421.
29. Gurian PL, Cheatham LK, Ziller JW, Barron AR (1991) *J Chem Soc Dalton Trans*, 1449–1456.
30. Atwood DA, Jegier JA, Rutherford D (1996) *Inorg Chem* 35:63–70.
31. Atwood DA, Hill MS, Jegier JA, Rutherford D (1997) *Organometallics* 16:2659–2664.
32. Atwood DA, Harvey MJ (2001) *Chem Rev* 101:37–52.
33. Addison AW, Rao TN, Reedijk J, van Rijn J, Verschoor GC (1984) *J Chem Soc Dalton Trans*, 1349–1356.
34. Dove AP, Gibson VC, Marshall EL, Rzepa HS, White AJP, Williams DJ (2006) *J Am Chem Soc* 128:9834–9843.
35. Marshall EL, Gibson VC, Rzepa HS (2005) *J Am Chem Soc* 127:6048–6051.